

RESEARCH ARTICLE

Mixotrophic microbes create carbon tipping points under warming

Daniel J. Wiczynski¹  | Holly V. Moeller²  | Jean P. Gibert¹ ¹Department of Biology, Duke University, Durham, North Carolina, USA²Department of Ecology, Evolution, and Marine Biology, University of California, Santa Barbara, California, USA**Correspondence**

Daniel J. Wiczynski

Email: daniel.wiczynski@duke.edu**Funding information**

National Science Foundation, Grant/Award Number: OCE-1851194; Simons Foundation, Grant/Award Number: 689265; U.S. Department of Energy, Grant/Award Number: DE-SC0020362

Handling Editor: Jianjun Wang**Abstract**

1. Mixotrophs are ubiquitous and integral to microbial food webs, but their impacts on the dynamics and functioning of broader ecosystems are largely unresolved.
2. Here, we show that mixotrophy produces a unique type of food web module that exhibits unusual ecological dynamics, with surprising consequences for carbon flux under warming. We develop a generalizable model of a mixotrophic food web module that incorporates dynamic switching between phototrophy and phagotrophy to assess ecological dynamics and total system CO₂ flux.
3. We find that warming switches mixotrophic systems between alternative stable carbon states—including a phototrophy-dominant carbon sink state, a phagotrophy-dominant carbon source state and cycling between these two. Moreover, warming always shifts this mixotrophic system from a carbon sink state to a carbon source state, but a coordinated increase in nutrients can erase early warning signals of this transition and expand hysteresis.
4. This suggests that mixotrophs can generate critical carbon tipping points under warming that will be more abrupt and less reversible when combined with increased nutrient levels, having widespread implications for ecosystem functioning in the face of rapid global change.

KEYWORDS

alternative stable states, carbon flux, climate change, ecosystem functioning, food webs, mixotrophy, tipping points

1 | INTRODUCTION

Microbial organisms play a critical role in ecosystem carbon and nutrient cycling (Geisen et al., 2020; Kayranli et al., 2010; Rocca et al., 2022; Schimel & Schaeffer, 2012; Steinberg & Landry, 2017; Zhang et al., 2018) that is likely to change with rapidly shifting global conditions (Bradford et al., 2019; Geisen et al., 2021; Smith et al., 2019; Wiczynski et al., 2021; Zhou et al., 2012). Understanding the net impacts of global change on ecosystem flux requires untangling the roles of a diverse assortment of ecological strategies

within the microbial world (Bengtsson et al., 1996; Gao et al., 2019; Geisen et al., 2020; Kuppardt-Kirmse & Chatzinotas, 2020; Petchey et al., 1999; Thakur & Geisen, 2019).

Mixotrophy is a common strategy within microbial communities, but its impacts on ecosystem processes and dynamics remain relatively unresolved (Esteban et al., 2010; Flynn et al., 2019; Jassey et al., 2015; Jones, 2000; Mitra et al., 2014; Moeller et al., 2019; Sanders, 1991; Selosse et al., 2017; Stoecker et al., 2017). Mixotrophs are organisms that combine two or more energy/carbon/electron acquisition (or trophic) modes—including several different forms of

autotrophy and heterotrophy (Eiler, 2006; Esteban et al., 2010; Flynn et al., 2013; Mitra et al., 2016; Stoecker, 1998; Stoecker et al., 2017; Yafremava et al., 2013). Although mixotrophy also occurs in plants (Schmidt et al., 2013; Selosse & Roy, 2009) and animals (Graham et al., 2013; Orr, 1888; Venn et al., 2008), the majority of mixotrophs are microorganisms like bacteria, archaea, protists and fungi (Selosse et al., 2017). Mixotrophic microbes are ubiquitous in terrestrial, freshwater and marine systems (Esteban et al., 2010; Flynn et al., 2019; Mieczan, 2009; Sanders, 1991; Selosse et al., 2017; Stoecker, 1998; Stoecker et al., 2017; Worden et al., 2015), and mixotrophy is increasingly recognized as a dominant energy acquisition strategy within microbial food webs (Eiler, 2006; Jassey et al., 2015; Mitra et al., 2014; Sanders, 1991; Selosse et al., 2017). By acting as both primary producers and consumers, mixotrophs play a unique role in ecosystem carbon and nutrient cycling (Jassey et al., 2015; Jones, 2000; Mitra et al., 2014) that is likely to change with warming (Wilken et al., 2013). Elucidating mixotrophic responses to rapidly changing environmental conditions is thus essential for understanding and predicting the impacts of global climate change on ecosystem functioning.

Here we focus on mixotrophic protists, which can combine autotrophy (particularly phototrophy) and heterotrophy (particularly phagotrophy of bacterial prey) in multiple ways according to the differential utilization of three basic resources—light, nutrients and prey organisms (Jones, 1997; Mitra et al., 2016; Stoecker, 1998). Mixotrophic protists generally fall into one of three categories: (1) ‘ideal’ mixotrophs that use phototrophy and phagotrophy equally well, (2) ‘phagotrophic algae’ that are primarily phototrophic but use phagotrophy when either light or nutrients are limiting and (3) ‘photosynthetic protozoa’ that are primarily phagotrophic but use phototrophy when prey are limiting or to supplement carbon needs. Importantly, the relative use of phototrophy and phagotrophy for resource acquisition is not fixed in any of these strategies. Indeed, changes in the availability of light, nutrients or prey can cause individual organisms to shift from one mode of energy acquisition to another (Stoecker, 1998).

Consequently, mixotrophy likely represents a unique type of food web module (a fundamental subcomponent of a larger food web [McCann & Gellner, 2012]) whose structural and dynamical qualities vary in response to shifts between energy acquisition modes by mixotrophs. Based on their underlying physiology, some mixotrophs may benefit more from phototrophy under certain conditions, acquiring carbon primarily via photosynthesis rather than predation (Figure 1, left). Under other conditions, phagotrophy may be favoured and carbon acquired primarily via prey (Figure 1, right). Importantly, mixotrophs may dynamically switch between these energy acquisition modes as conditions change across space or time. This dynamic blending of energy acquisition modes could introduce novel dynamical regimes, altering population dynamics, species interactions and the stability of ecological communities in ways that are not fully captured by current theoretical frameworks. Although some studies have investigated mixotrophic dynamics using mathematical models (e.g. Jost et al., 2004; Moeller et al., 2016, 2019;

Moroz et al., 2019; Thingstad et al., 1996; Yang et al., 2016), these tend to be tailored to specific systems, organisms and environmental conditions, potentially missing the full range of dynamical behaviours possible in mixotrophic systems. To begin to explore these possible behaviours—and how they are altered by environmental change—we need generalizable mixotrophic models that incorporate dynamically shifting resource acquisition modes in response to changes in the availability of resources and variation in environmental conditions. Such models will allow us to better understand the ecological mechanisms underlying the diverse roles of mixotrophs within food webs, their associated impacts on ecosystem functioning, and their responses to environmental change.

Additionally, the processes that control mixotrophic population dynamics—autotrophic production (photosynthesis), heterotrophic production (predation), respiration, mortality, etc.—are expected to be accelerated by warming (Allen et al., 2005; Brown et al., 2004; Dell et al., 2014; Savage et al., 2004), but may exhibit different sensitivities to temperature change. Importantly, autotrophic production exhibits significantly lower sensitivity to increasing temperature than heterotrophic production, as evidenced by temperature sensitivities (in the form of ‘activation energies’) of ~ 0.32 eV and ~ 0.65 eV respectively (Allen et al., 2005; López-Urrutia et al., 2006; Yvon-Durocher & Allen, 2012). Consequently, some empirical (Wilken et al., 2013, 2018) and theoretical (Yang et al., 2016) evidence suggests that mixotrophs will tend to favour heterotrophy over autotrophy with warming. But whether this transition will be sudden or gradual, and whether this will be mediated by other environmental change factors (e.g. eutrophication), is virtually unknown.

Here we develop a generalizable mixotrophic food web model to evaluate the impacts of environmental change on mixotrophic dynamics and carbon flux. We address three main questions: (1) Does environmental change (in the form of temperature and nutrient concentration) alter the ecological dynamics and stability of mixotrophic systems?, (2) Does this, in turn, cause shifts in carbon flux states (i.e. carbon sink and carbon source states)? and (3) Are there early warning signals for tipping points between these states? Our results show that mixotrophic systems undergo complex—but predictable—dynamical transitions between alternative stable carbon states with warming that may be preceded by early warning signals in the form of steady-state cycling behaviour. However, these early warning signals disappear and are replaced by an abrupt carbon state shift when warming is accompanied by increasing nutrient levels, which has important implications for ecosystem functioning in a rapidly warming and increasingly anthropogenized world.

2 | MATERIALS AND METHODS

2.1 | Mixotrophic model

The physiological processes that underlie switching between trophic modes in different types of mixotrophs can be modelled by defining specific dependencies (functional responses) of photosynthesis

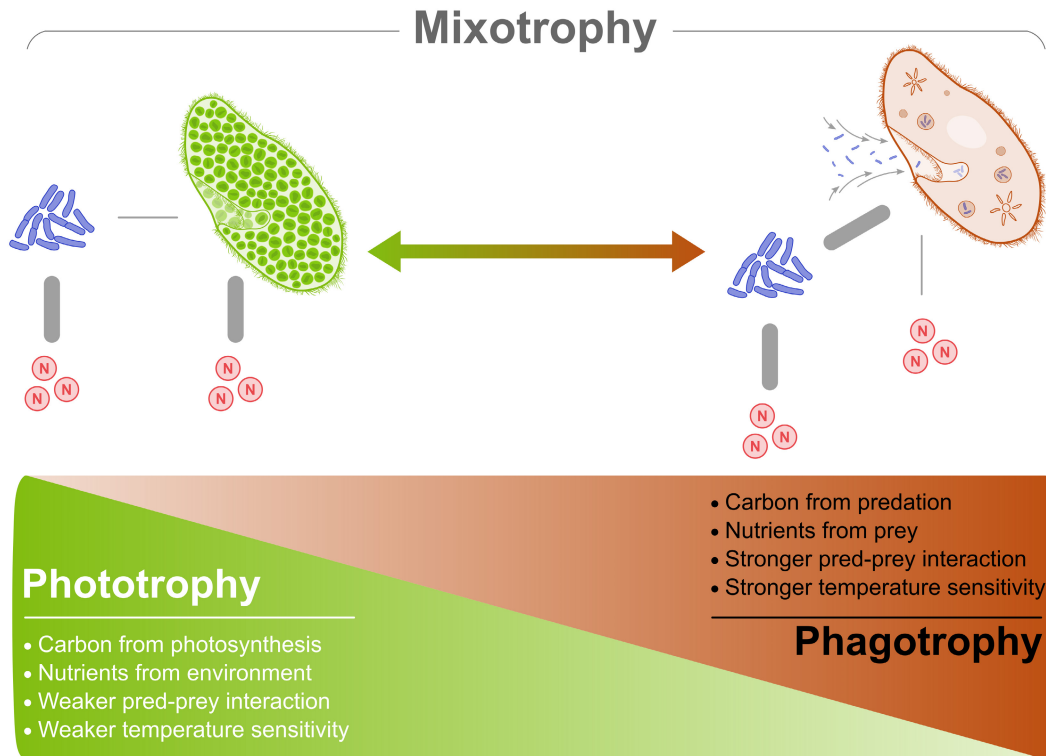


FIGURE 1 Mixotrophs move dynamically along a spectrum of carbon/energy acquisition modes between phototrophy and phagotrophy according to changes in the environment and three essential resources: nutrients, prey or light. A mixotrophic protist is shown here with its prey (bacteria; blue) and their respective essential nutrients (N). When phototrophy dominates, carbon is obtained primarily via photosynthesis, nutrients come from the environment, and the mixotroph occupies the same trophic level as its prey. When phagotrophy dominates, carbon and nutrients are obtained primarily via predation and the mixotroph occupies a higher trophic level than its prey. As mixotrophs switch between phototrophy and phagotrophy, the mixotrophic food web module shifts between single-species dynamics (or competition, if the mixotroph shares a resource with its prey) and predator-prey dynamics respectively. The dynamic nature of the mixotrophic food web module likely impacts the structure and dynamics of food webs as well as the flux of matter and energy in broader ecosystems.

and predation on three limiting resources: prey, nutrients and light (Stoecker, 1998). To study the effects of warming, we also incorporate temperature dependence on several rate parameters in our model. We focus our analysis on a model of mixotrophy representing organisms that are primarily phagotrophic but switch to photosynthesis to obtain carbon when prey are limiting (known as 'photosynthetic protozoa', or Type-IIIA mixotrophs in the terminology of Stoecker, 1998; Figure S1). Although we study this particular type of mixotroph here, our model can be generalized to any other type of mixotrophs by replacing the functional responses for prey, nutrient and light dependencies with alternative functional forms (e.g. a Type-IIA 'phagotrophic algae' mixotroph is analysed in Figure S2).

Our mixotrophic model consists of two ordinary differential equations (ODEs) that define the dynamics of a two-species system—a mixotroph (M) and its prey (P):

$$\frac{dM}{dt} = M \left(\varphi(T, N_M, P, M) + \frac{\varepsilon \alpha(T) P}{1 + \alpha(T) \tau P} - \delta_M(T) - m_M(T) \right) \quad (1a)$$

$$\frac{dP}{dt} = P \left(\mu_P(T) \frac{N_P}{h_P + N_P} \left(1 - \frac{P}{K_P} \right) - \frac{\alpha(T) M}{1 + \alpha(T) \tau P} - \delta_P(T) - m_P(T) \right), \quad (1b)$$

where M and P are biomass densities in units of milligrams of carbon per litre (Table 1; these units produce biomass densities in our model that correspond with published densities of a common mixotrophic protist, *Paramecium bursaria*; Gibert et al., 2017, assuming an average cell mass of $1.19 \cdot 10^{-7}$ g Wieczynski et al., 2021). The mixotroph's per-capita biomass production rates from photosynthesis and predation are, respectively:

$$\text{Photosynthesis: } \varphi(T, N_M, P, M) = \mu_M(T) \frac{N_M}{h_M + N_M} e^{-dP^2} \left(1 - \frac{M}{K_M} \right) \quad (2a)$$

$$\text{Predation: } \lambda(T, P) = \frac{\varepsilon \alpha(T) P}{1 + \alpha(T) \tau P}. \quad (2b)$$

Photosynthetic production rate (φ) follows a modified logistic-growth form that incorporates dependencies on temperature (T), nutrient concentration (N_M ; we consider a generic limiting nutrient for generality because different mixotrophic species could be limited by different nutrients [Raven, 1997; Stoecker, 1998]), prey density (P) and mixotroph density (M). Per-capita photosynthetic production is assumed to decline as mixotroph density approaches a carrying capacity (K_M), due to limitation of essential resources (e.g. light). Nutrient uptake follows

Variable/ parameter	Definition	Units	Value
M, P	Biomass density	mg CL^{-1}	na
N_i	Nutrient concentration	mg L^{-1}	$N_M = [0.4, 1.0]$ $N_p = 0.7$
h_i	Half-saturation constant	mg L^{-1}	$h_M = 0.8$ $h_p = 0.3$
d	Photosynthesis prey dependence decline rate	$(\text{mg CL}^{-1})^{-2}$	0.072
K_i	Carrying capacity	mg CL^{-1}	$K_M = 10$ $K_p = 19$
ϵ	Max conversion efficiency	n/a	0.25
Temperature-dependent parameters (following Equation 2)			
$\mu_i(T)$	Max production rate	t^{-1}	$\mu_M(T): b_0 = 0.45; E_a = 0.32$ $\mu_p(T): b_0 = 1.35; E_a = 0.65$
$\alpha(T)$	Attack rate	t^{-1}	$b_0 = 0.21; E_a = 0.65$
$\delta_i(T)$	Respiration rate	t^{-1}	$\delta_M(T): b_0 = 0.07; E_a = 0.65$ $\delta_p(T): b_0 = 0.05; E_a = 0.65$
$m_i(T)$	Mortality rate	t^{-1}	$m_M(T): b_0 = 0.072; E_a = 0.45$ $m_p(T): b_0 = 0.052; E_a = 0.45$

TABLE 1 Variables and parameters used in the mixotrophy model.

Michaelis–Menten kinetics where uptake rate saturates with increasing nutrient concentrations to a maximum rate ($\mu_M(T)$) according to a half-saturation constant (h_M , i.e. the nutrient concentration at which the foraging rate is half the maximum possible rate). To capture a reduction in photosynthetic investment when prey are abundant, the dependence of photosynthetic production rate on prey density is defined by a declining function (e^{-dP^2}) that decreases with increasing prey density at a rate determined by d and saturates at a maximum value as prey density approaches zero (Figure S1a). Predation rate (λ) follows a type-II functional response that saturates with increasing prey density and has an attack rate of $\alpha(T)$ (for simplicity we assume that handling time $\tau = 1$). Biomass loss is accounted for through the parameters δ_M and m_M , which represent respiration and mortality respectively. The percentage of total production that comes from photosynthesis was calculated as $\varphi/(\varphi + \lambda) \cdot 100$.

Prey are assumed to be exclusively chemoheterotrophic and also follow a modified logistic form, with dependencies on temperature (T), prey-specific nutrient concentration (N_p) and prey density (P) defined by Michaelis–Menten kinetics with maximum uptake rate $\mu_p(T)$, a half-saturation constant h_p and carrying capacity K_p . Prey biomass declines through predation by the mixotroph (λ/ϵ), respiration (δ_p) and mortality (m_p). In our main analysis, prey nutrients (N_p) are held constant, but we consider variation in N_p in Supporting Information Figure S4, including the scenario where prey and mixotroph nutrients are the same (i.e. $N_p = N_M$), in which case our results are qualitatively the same.

2.2 | Temperature dependence

Maximum uptake, attack, mortality and respiration rates are all assumed to be temperature dependent (explicitly written as a function of T in Equations 1 and 2) and follow the common Arrhenius form:

$$\text{rate}(T) = b_0 e^{-\frac{E_a}{k} \left(\frac{1}{T} - \frac{1}{T_{\text{ref}}} \right)}, \quad (3)$$

where b_0 is a normalization constant, E_a is an ‘activation energy’ or temperature-sensitivity parameter (in eV), k is Boltzmann’s constant ($8.6 \cdot 10^{-5} \text{ eV} \cdot \text{K}^{-1}$) and T_{ref} is a reference temperature at which the given rate is equal to b_0 ($T_{\text{ref}} = 20^\circ\text{C}$ for all parameters in our model). The temperature sensitivities of each rate are controlled by the activation energies (E_a), which were empirically estimated elsewhere: $E_a = 0.32$ for photosynthetic production (Allen et al., 2005) and $E_a = 0.65$ for heterotrophic production and respiration (Brown et al., 2004; Dell et al., 2011). However, we also consider the scenario in which temperature sensitivities do not differ between photosynthetic and heterotrophic production rates (Figure S3).

2.3 | CO₂ flux

We study how changes in temperature affect the net CO₂ flux between our mixotrophic system and the atmosphere by ecologically altering the balance of photosynthesis and respiration. Our model focuses specifically on the direct exchange of CO₂ between organisms and the environment, but it should be noted that other sources of carbon (e.g. CH₄ or dead organic matter) could also contribute to carbon flux in a broader ecosystem context. Thus, our definition of CO₂ flux in this system should be considered as a local component within the greater carbon cycle. We also consider our prey species to be heterotrophic, but phototrophic prey could be incorporated by accounting for photosynthetic CO₂ uptake by the prey. To track the dynamics of CO₂ flux, we calculated net CO₂ flux as total system respiration rate minus total system photosynthetic rate:

$$\text{CO}_2 \text{ flux} = 3.67 * (\delta_M(T)M + \delta_P(T)P - \varphi(T, n, P, M)M), \quad (4)$$

where $\delta_M(T)M + \delta_P(T)P$ is total system respiration rate and the third term $\varphi(T, n, P, M)M$ represents the rate of carbon uptake for use in photosynthesis. The coefficient 3.67 converts grams of carbon (C) to grams of carbon dioxide (CO_2) ($\text{gCO}_2/\text{gC} = 44/12 = 3.67$).

2.4 | Equilibria and stability analysis

We quantified equilibria by setting parameters equal to the values in Table 1, setting Equations 1a–1b equal to zero, and solving the system for both state variables (using the 'Solve' function in Mathematica V13.0.0 [Wolfram Research, Inc., 2021]) across a range of temperatures (19–23°C) and concentrations of the limiting nutrient for the mixotroph (0.4–1.0 mg L^{-1} ; this range corresponds with known concentrations of nutrients like nitrate and phosphate in peatland habitats where mixotrophs are commonly found [Mieczan, 2009]). These environmental parameter ranges were chosen because they encompass the full range of possible alternative stable states for the parameter values listed in Table 1. Our main analysis considers static nutrients, however, in the Supporting Information we also consider dynamic nutrients (Figure S5) as well as variation in nutrients that limit the prey (Figure S4). Null clines (Figure 2a–c) were calculated for each species by setting per-capita growth rates equal to zero and solving for M : Mixotroph null cline, $M = K_M \left(1 + \frac{h_M + N_M}{\mu_M(T)N_M} e^{dP^2} \left(\frac{\epsilon\alpha(T)P}{1 + \alpha(T)rP} - \delta_M(T) - m_M(T) \right) \right)$; Prey null cline, $M = \frac{1 + \alpha(T)rP}{\alpha(T)} \left(\mu_P(T) \frac{N_P}{h_P + N_P} \left(1 - \frac{P}{K_P} \right) - \delta_P(T) - m_P(T) \right)$. The stability and dynamical behaviour of equilibria were determined through local stability analysis, that is, by calculating the eigenvalues (for our system there are two, one for each state variable) of the Jacobian matrix evaluated at equilibrium in each environmental state (i.e. combination of temperature and nutrient concentration), then using those eigenvalues to characterize the stability of equilibria. Equilibria with eigenvalues that only have real parts are nonoscillatory and can either be (i) a stable node if both eigenvalues are negative, (ii) an unstable node if both eigenvalues are positive or (iii) an unstable saddle point if the eigenvalues have opposite signs. Equilibria with complex eigenvalues (i.e. that include imaginary parts) can either be (i) a stable focus (inward spiral) when the real parts are negative or (ii) an unstable focus (outward spiral) when the real parts are positive. In addition to these fixed point equilibria, there may be closed trajectories within state space called 'limit cycles' that neighbouring trajectories either spiral towards (stable limit cycle) or away from (unstable limit cycle) as time approaches infinity. We refer to both stable fixed points and stable limit cycles as 'attractors'. Attractors were identified by numerically solving the system for 100,000 time steps and recording the maximum and minimum densities of each species for the last 10,000 time steps. We repeated this process for all equilibria in each environmental state, initializing each numerical solution with small perturbations from each equilibrium point (equilibrium values + 0.001).

This allowed us to evaluate long-term, stationary dynamics created by stable limit cycles. To evaluate how sensitive this system is to variation in parameter values, we also conducted a sensitivity analysis in which each of the parameters in our model (Table 1) was increased/decreased by 25% and equilibria and steady-state trajectories were calculated across a wide range of temperatures (16–26°C; Figure S6).

3 | RESULTS

3.1 | Effects of temperature on mixotrophic dynamics

Increasing temperature reshapes the dynamical landscape of this mixotrophic system (Figure 2). At low temperatures, a single, stable fixed point exists where mixotrophs are at an intermediate density and their prey are at very low (or zero) density (Figure 2a, green). At intermediate temperatures, three attractors co-occur: (i) one stable fixed point where both species are at relatively low densities (green), (ii) one high-density stable fixed point (orange) and (iii) a stable limit cycle that orbits these two stable points (blue; Figure 2b). At higher temperatures, only one stable fixed point exists where both species coexist at relatively high densities (Figure 2c). At very low and high temperatures, only single-species stable fixed points exist, where either the mixotroph (at low temperatures) or the prey (at high temperatures) persists alone (i.e. no coexistence).

Transitions between these attractors are produced by a progression of bifurcations across temperatures (Figure 2d). Multiple equilibria exist across a range of intermediate temperatures (20.06–21.99°C) whose stability and dynamical behaviour change as temperature increases. First, an unstable focus (black dashed line) and an unstable saddle point (grey dotted line) appear at 20.06°C, in addition to the original stable fixed point (green line), and the long-term dynamics approach this stable point regardless of initial conditions (Figure 2d). Next, at 20.7°C multiple attractors co-occur—one is the original stable fixed point (green) and the other is a stable limit cycle (blue lines, grey shading) that orbits the stable and unstable fixed points. The high-density stable fixed point (orange) appears at 20.79°C, producing a unique form of tri-stability including all three of the different attractors described above (Figure 2b). In this case, cycling will only occur if the initial conditions are sufficiently far away from either stable fixed point, otherwise the system will approach one of these stable fixed points. The stable limit cycle disappears at 21.05°C, leaving two stable fixed points, but the low-density stable fixed point (green) quickly becomes an unstable focus at 21.1°C, at which point long-term trajectories always approach the high-density stable fixed point (orange). Eventually, as temperature increases to 22°C, only one, high-density stable fixed point (orange) remains (Figure 2c). In short, increasing temperature produces a transition between alternative stable states (Figure 2, green and orange) that overlap

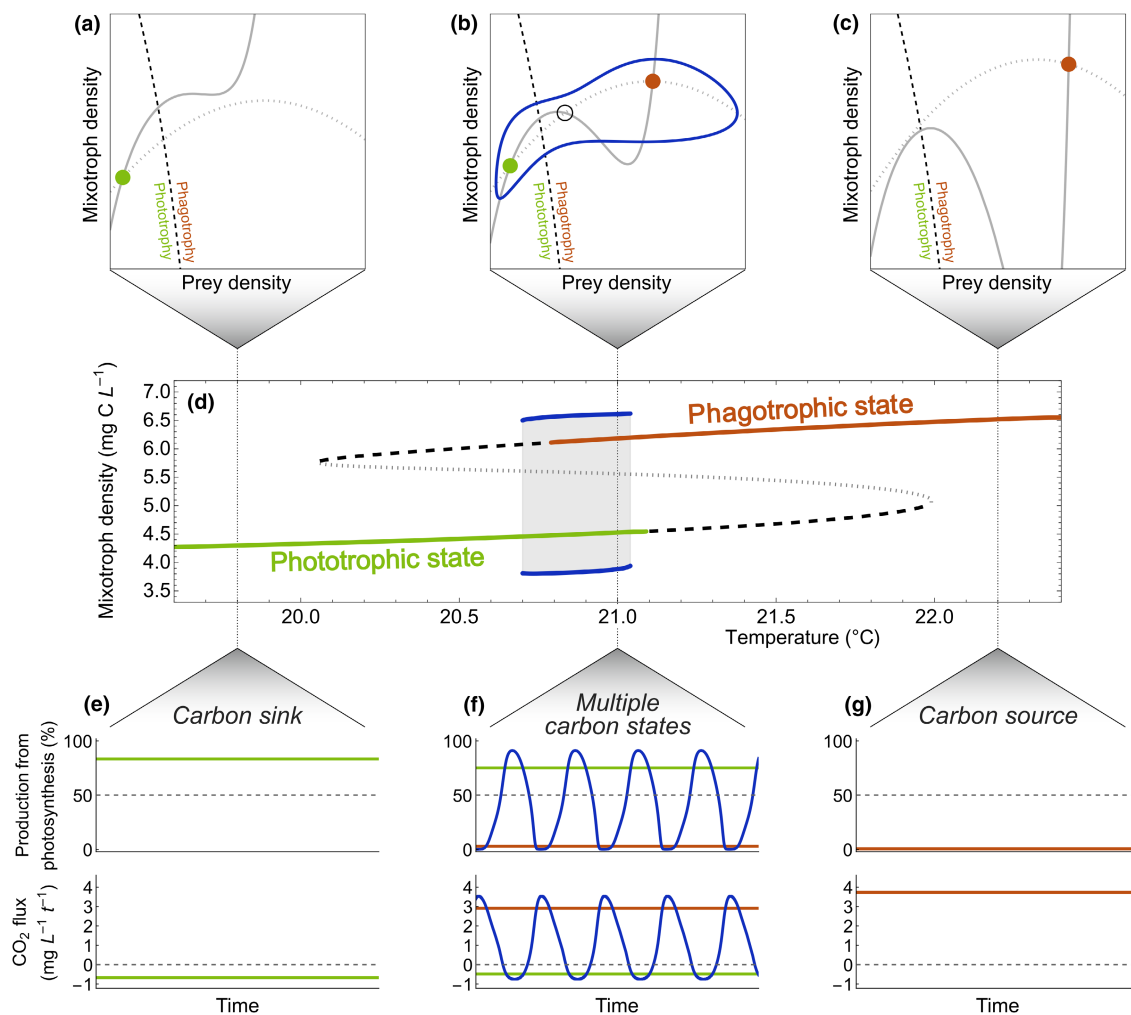


FIGURE 2 Increasing temperature shifts equilibrium densities, the balance between phototrophy and phagotrophy, and net CO₂ flux. (a–c) Phase portraits displaying null clines (grey lines) for the prey species (dotted) and the mixotrophic species (solid). Intersections of these null clines represent equilibrium points that are either stable (solid green and orange dots) or unstable (open circle). The blue lines indicate stable limit cycles that orbit the three interior equilibria. The black dashed line separates a region where phototrophy dominates production (left) from a region where phagotrophy dominates production (right). (d) A bifurcation diagram displaying transitions between equilibrium scenarios as a function of increasing temperature. (a), (b) and (c) correspond to temperatures of 19.8°C, 21.0°C and 22.2°C respectively. (e–g) Long-term dynamical behaviour of the percentage of production from photosynthesis in the mixotroph and the total system net CO₂ flux at 19.8°C, 21.0°C and 22.2°C respectively. Colours correspond to stable equilibria and limit cycles in (a–d). Results here assume intermediate nutrient concentrations $N_M = 0.7 \text{ mg L}^{-1}$.

at intermediate temperatures, where stable cycling around these states may also occur (Figure 2, blue).

3.2 | Effects of temperature on carbon flux

Increasing temperature shifts this mixotrophic system from a net carbon sink (phototrophic state dominated by photosynthesis; Figure 2e), through multiple possible carbon states (sink or source; Figure 2f), to a net carbon source (phagotrophic state dominated by predation; Figure 2g). This sequence of carbon state transitions corresponds with changes in the dominant carbon acquisition strategy of the mixotroph. At low temperatures, most of the mixotroph's biomass production comes from

photosynthesis and, after accounting for carbon uptake for use in photosynthesis and carbon release through respiration by both species, the net flux of carbon dioxide (CO₂) in the system is negative (i.e. a net carbon sink; Figure 2e). At intermediate temperatures, three possible carbon states co-occur: (i) one carbon sink state (green), (ii) one fluctuating state where production cycles between photosynthesis and predation and the system fluctuates between being a carbon sink and carbon source respectively (blue) and (iii) one carbon source state where production is dominated by predation and net carbon flux is positive (Figure 2f). At high temperatures, predation takes over as the sole form of production and the system becomes an exclusive net carbon source (Figure 2g). Because fluctuations span a range of intermediate temperatures separating carbon sink and source

states (Figure 2d), these fluctuations can be considered an early warning signal of this transition.

3.3 | Combined effects of temperature and nutrient concentration

The temperature-driven progression between alternative stable states is mediated by nutrient concentration (Figure 3). Changes in

temperature and nutrient levels lead to a complex equilibrium landscape that produces a rich assortment of behaviours (Figure 3a). Within this landscape, the range of temperatures producing multiple nontrivial equilibria widens with increasing nutrient concentration (Figure 3a; region inside solid black line), creating upper and lower equilibrium branches in three-dimensional space (Figure 3b) consisting of various combinations of stable and unstable fixed points that are separated by an interior branch of unstable saddle points (Figure 3a).

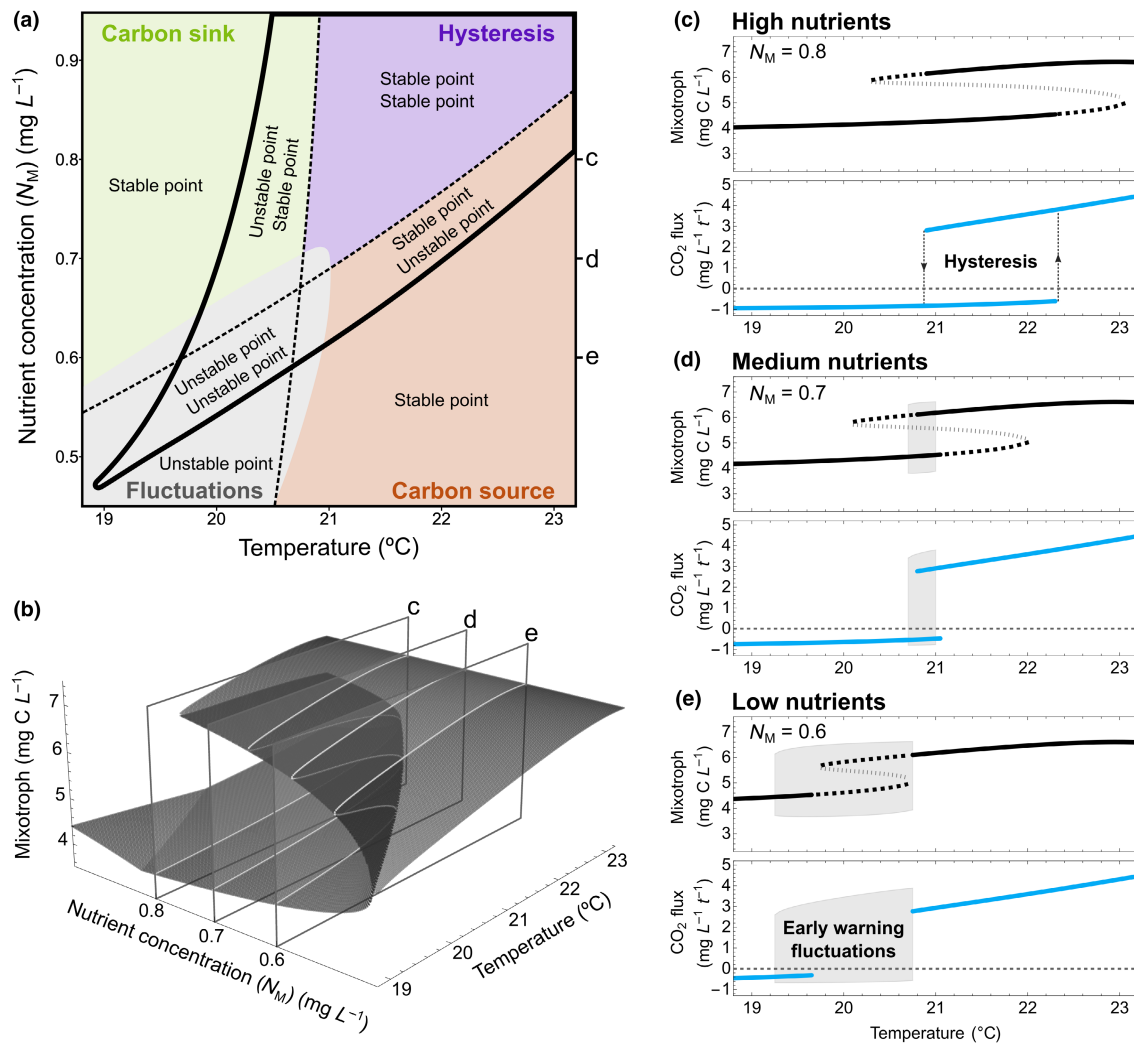


FIGURE 3 Gradients in temperature and nutrient concentrations produce a rich landscape of equilibrium behaviours. (a) Different environmental conditions produce different equilibrium scenarios with different combinations of stable and unstable fixed points (the solid black line delineates regions with one (outside) or multiple (inside) co-occurring equilibria and black dashed lines further subdivide these regions). For regions with multiple equilibria, the upper and lower text correspond to the orientation of upper and lower equilibria in three-dimensional space (b) (note that these upper and lower equilibria are always separated by an unstable saddle point). The steady-state carbon flux behaviours of each equilibrium scenario are shown in coloured regions: static carbon sink (green), static carbon source (orange), fluctuations between carbon sink and source states (grey) and hysteresis with overlapping, static carbon sink and source states (purple). Note that carbon state fluctuations (grey) can occur even in the presence of stable points, even without an unstable point present. (b) In three-dimensional space, equilibria create a folded landscape where the upper and lower branches are either stable or unstable points and are separated by an interior branch of unstable saddle points. (c–e) show bifurcation diagrams of equilibrium densities (upper panels) and steady-state CO_2 flux (lower panels, unstable equilibria not shown) across temperatures for three different nutrient concentrations (indicated by 'c', 'd' and 'e' in panels (a) and (b)). Solid lines (black and blue) denote stable point equilibria, dashed lines denote unstable foci, grey regions denote stable limit cycles (fluctuations) and dotted lines denote unstable saddle points (i.e. the interior branch in (b)).

The carbon flux behaviour of a mixotrophic system in any given environmental state (i.e. combination of temperature and nutrients) depends on the arrangement of these equilibria (Figure 3a). A static carbon sink state can occur within a region of low temperatures and high nutrient concentrations, where either a single, stable fixed point exists alone (at low mixotroph density) or this stable fixed point in the lower branch is accompanied by an unstable focus in the upper branch (Figure 3a, green). Conversely, a static carbon source state occurs when temperatures are higher and nutrient concentrations are lower, associated with either a single, stable, high-mixotroph-density stable fixed point in the upper branch that is either alone or accompanied by an unstable focus in the lower branch (Figure 3a, orange). Interestingly, stable limit cycles can occur under any combination of fixed points, producing fluctuations in carbon flux between carbon sink and source states (Figure 3a, grey). In some cases, stable limit cycles can occur around stable fixed points, even without an unstable fixed point present (see Section 4 for more information). At high temperatures and nutrient concentrations, hysteresis results because only static, stable carbon sink and source states occur together (Figure 3a, purple).

3.4 | Early warning signals for transitions between carbon flux states

Interestingly, increasing nutrient loads erases early warning signals of a shift between carbon sink to carbon source states with warming (Figure 3c–e). Early warning signals come in the form of fluctuations in carbon flux (produced by a stable limit cycle) between carbon sink and source states that precede the transition to a static carbon source state as temperature increases (grey region in Figure 3a). Indeed, at low nutrient concentrations ($N_M = 0.6 \text{ mg L}^{-1}$), increasing temperatures produces a large temperature window over which fluctuations in carbon flux occur before the system eventually locks in to a static carbon source state (Figure 3e). As nutrient concentration increases, the range of temperatures that produce fluctuations shrinks (grey region in Figure 3a) and alternative stable fixed points begin to

overlap at intermediate temperatures (e.g. as in Figure 3d). When nutrient concentrations become high enough, fluctuations completely disappear and static alternative stable carbon states overlap across a wide range of temperatures (i.e. hysteresis; Figure 3a,c). In this case, the warming-induced tipping point to a static carbon source state is abrupt and occurs without warning. Additionally, once warming has shifted the system to a carbon source state, a significant reduction in temperature ($>1^\circ\text{C}$) would be required to revert the system back to the carbon sink state (Figure 3c).

Generally speaking, although warming always leads to a transition from a carbon sink state to a carbon source state, whether this transition is preceded by a period of fluctuating carbon flux dynamics (early warning signal) depends on nutrient concentrations. Moreover, increasing nutrients reduces the temperature range over which fluctuating carbon flux dynamics occur (shortening early warning signals) while also increasing the temperature range over which static carbon sink and source states overlap (widening hysteresis) (Figures 3a and 4).

4 | DISCUSSION

Mixotrophic organisms and their prey can be considered a unique type of food web module that dynamically transitions between a phototrophy-dominant single-species or competition module and phagotrophy-dominant consumer-resource module, generating surprising dynamical behaviours that can have important—albeit largely unknown—impacts on ecosystem functioning in novel environments. Here we show how warming can shift mixotrophic systems from a photosynthesis-dominant net carbon sink state (Figure 2a,e) to a predation-dominant net carbon source state (Figure 2c,g). These transitions are preceded by early warning signals in the form of fluctuations between carbon source and sink states when nutrient concentrations are low (Figure 3a,e), but increasing nutrients erases these early warning signals by replacing fluctuations with overlapping static carbon sink and source states (hysteresis; Figure 3a,c). Taken together, this suggests that mixotrophic systems could shift from

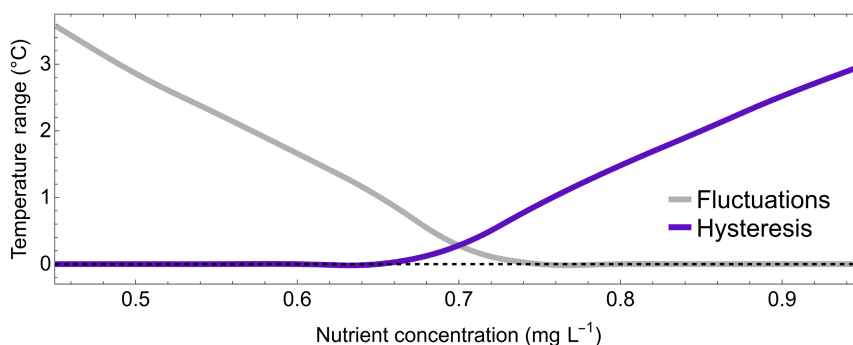


FIGURE 4 The effect of nutrient concentration on the range of temperatures over which fluctuations in carbon flux (an early warning signal of a carbon tipping point) and overlapping static carbon sink and source states (hysteresis) occur. The decline in fluctuations with increasing nutrients (grey) indicates a reduction in the temperature window producing early warning signals. Increases in the range of temperatures where stable carbon states overlap (purple) indicates increasing hysteresis. Dashed line indicates a temperature range of 0.

carbon sinks to carbon sources with warming and this transition may be more abrupt and less reversible when combined with increased nutrient levels. Given the ubiquity of mixotrophs across all types of ecosystems (Flynn et al., 2019; Mieczan, 2009; Sanders, 1991; Selosse et al., 2017; Stoecker, 1998; Stoecker et al., 2017; Worden et al., 2015), our results uncover a potentially crucial but previously unknown aspect of ecosystem responses to global change.

Ecologists have been concerned about identifying how changing environmental conditions might produce tipping points and abrupt regime shifts for decades (Dakos et al., 2019; Dakos & Hastings, 2013; Folke et al., 2004; Holling, 1973; May, 1977; Scheffer et al., 2001, 2009). Our study exposes a new mechanism by which abrupt regime shifts may occur—through the unique dynamics of mixotrophic organisms. We find that early warning signals of such shifts may occur in the form of deterministic fluctuating dynamics that are intrinsic to the mixotrophic system and bridge a transition between static carbon sink and carbon source states. These fluctuations are distinct from another form of fluctuating early warning signal called ‘stochastic flickering’ where stochastic variability can shift the system between alternative static states (Scheffer et al., 2009), which could also potentially occur in our system in the absence of the deterministic fluctuations found here (e.g. Figure 3c). However, we also find that these early warning signals may be environmentally context dependent—the nature of regime shifts across one environmental gradient might depend on the state of separate environmental factors (as is also evident in some empirical examples of regime shifts [Folke et al., 2004]). In our system, the window of early warning signals with warming (e.g. fluctuations spanning temperature changes of $\sim 0.25^\circ\text{C}$ vs $\sim 1.5^\circ\text{C}$ in Figure 3d,e respectively), and indeed their very existence (e.g. the lack of fluctuations in Figure 3c), depends on coordinated changes along multivariate environmental gradients (temperature and nutrient concentrations in our case), which could shed light on why tipping points are so elusive in nature (Connell & Sousa, 1983; Dudney & Suding, 2020; Hillebrand et al., 2020). We propose that, in addition to providing potentially critical early warnings for carbon tipping points under climate change, mixotrophs also represent an opportunity to study complex regime shifts and variation in early warning signals across multivariate environmental gradients.

There is growing recognition that temperature and nutrients interact to impact the structure and dynamics of ecological communities (Binzer et al., 2012, 2016; Gilbert et al., 2014; Han et al., 2023; Sentis et al., 2014). Discovering conditions under which temperature–nutrient interactions occur and which properties of ecological systems are affected (e.g. species extinction risk, food web structure and stability, etc.) is of particular interest. In our model, nutrient levels mediate the impacts of warming on carbon flux dynamics and also determine our ability to predict abrupt transitions between alternative carbon flux states. The critical condition producing this previously unrecognized temperature–nutrient interaction is the dynamic balancing of carbon uptake (via photosynthesis) and carbon release (via respiration) due to flexible energy

acquisition strategies in mixotrophs. However, it is possible that the temperature–nutrient interaction studied here might extend beyond mixotrophic systems to other multispecies systems that also dynamically balance carbon uptake and release (i.e. systems that include both autotrophs and heterotrophs). Determining the generality of this type of temperature–nutrient interaction is an interesting question and area for future research.

The mixotrophic system studied here produces dynamical behaviours that are highly unusual in ecological systems. Specifically, our model produces a unique form of tri-stability—two alternative stable fixed points and stable cycling around these points (Figures 2b and 3d)—with important associated impacts on carbon flux dynamics. Another example of unusual behaviour occurs when nutrient concentration is low (Figure 3e): some temperatures (19.24 – 19.65°C) produce a stable limit cycle around a single fixed point (i.e. a single stable focus that is encircled by two limit cycles—one outer, stable limit cycle and one inner, unstable limit cycle). In this situation, the system can produce two possible long-term behaviours: (i) dampened oscillations towards the stable focus point when initial conditions are inside the inner, unstable limit cycle or (ii) cycling around this stable point when initial conditions are outside the unstable limit cycle. This specific arrangement of coexisting attractors is known to occur in nonecological systems (De Carvalho Braga & Mello, 2013), but seems to be exceedingly rare in ecological systems (but see Erbach et al., 2013; Tyson & Lutscher, 2016). The dynamics in each of these examples are a direct result of the flexible carbon acquisition strategies of mixotrophs and variation in environmental conditions, suggesting that other unusual dynamics are possible, or even common, in mixotrophic systems and probably vary across environments. Hence, investigating the dynamical behaviours of mixotrophic systems could fundamentally change our understanding about the dynamics and structure of microbial communities as well as ecosystem responses to global change.

Our study focuses on a specific type of mixotrophic organism—a primarily predatory organism that uses photosynthesis to supplement energy needs when prey densities are low (i.e. ‘photosynthetic protozoa’ in the language of Stoecker, 1998). But several different types of mixotrophic organisms exist, exhibiting a wide range of mixotrophic strategies and responses to changes in light, nutrient concentrations and prey densities (Jones, 1997; Mitra et al., 2016; Stoecker, 1998). Each type of mixotroph is likely to produce unique dynamical responses to changes in environmental conditions with different associated impacts on carbon flux. As such, mixotrophs may cause a rich array of novel dynamics that have yet to be uncovered either theoretically or empirically. Although our main analysis is based on one specific type of mixotroph (‘photosynthetic protozoa’), we designed our modelling framework so that it can easily be extended to incorporate the specific resource dependencies of any type of mixotroph simply by defining functional responses for light availability, nutrient concentrations and prey densities as desired (see Supporting Information for details). For example, in Figure S2 we altered these functional responses to create a very different type of mixotroph called ‘phagotrophic algae’ that is primarily

phototrophic but eats prey to supplement nutrient needs for photosynthesis (Stoecker, 1998). Interestingly, increasing temperature can produce hysteresis between carbon sink and source states in this type of mixotroph, too (Figure S2). While these results show that temperature-driven alternative carbon states may be robust across different types of mixotrophs, there is still much to learn about how the variety of different mixotrophs may respond to global change.

Our analysis makes several other assumptions regarding the particular sort of mixotrophic system studied here: two-species system, heterotrophic prey, static nutrient concentrations, single limiting nutrient, fixed stoichiometry, static environments, specific temperature sensitivities, etc. For example, our main analysis considers a specific set of fixed values for several parameters (Table 1). We explored the effects of variation in all model parameters using a sensitivity analysis and found that temperature-driven alternative stable state transitions can occur across a wide range of parameter space, meaning that the phenomena observed in our main analysis could occur in a variety of mixotrophic scenarios (Figure S6). We also assumed that phototrophic and heterotrophic production rates exhibit different temperature sensitivities (photo=0.32 eV, hetero=0.65 eV). However, we found that these differences are not actually necessary to produce temperature-driven transitions between carbon sink and source states (Figure S3). Instead, abrupt changes in mixotrophic production modes and species' production rates and densities may be sufficient to tip the net balance of photosynthesis and respiration towards a carbon source state even without differences in photo- and heterotrophic temperature sensitivities. In our analysis, we assumed that both species were nutrient-limited with nutrients held at static concentrations, but we found that our results are robust to the inclusion of nutrient dynamics, too (Figure S5). Additionally, we focused only on the effects of variation in nutrients utilized by the mixotroph species, however, increasing prey nutrients may mitigate, or even reverse, the transitions between carbon flux states with warming (Figure S4). Furthermore, it remains unclear how explicit competition for resources between a mixotroph and its prey might impact carbon flux. Relaxing these and other assumptions could have myriad consequences for dynamics that should be explored in future studies.

Overall, we show that these globally distributed (Esteban et al., 2010; Flynn et al., 2019; Mieczan, 2009; Sanders, 1991; Selosse et al., 2017; Stoecker, 1998; Stoecker et al., 2017; Worden et al., 2015) and massively abundant (Bar-On et al., 2018) mixotrophic microbes exhibit a rich array of dynamical responses to joint changes in temperature and nutrient levels, leading to fundamentally important tipping points between carbon flux states. We also show that nutrient levels determine whether these carbon tipping points are abrupt or accompanied by early warning signals, which is of paramount importance in a rapidly warming and increasingly human-influenced world.

AUTHOR CONTRIBUTIONS

Daniel J. Wiczynski designed the study and performed the mathematical modelling with support from Holly V. Moeller and Jean P.

Gibert. Daniel J. Wiczynski wrote the first draft of the manuscript and all authors contributed substantially to revisions.

ACKNOWLEDGEMENTS

H.V.M. was supported by a grant from the Simons Foundation (Award Number 689265) and NSF Award OCE-1851194. D.J.W. and J.P.G. were supported by a U.S. Department of Energy, Office of Science, Office of Biological and Environmental Research, Genomic Science Program Grant award to J.P.G., under Award Number DE-SC0020362.

CONFLICT OF INTEREST STATEMENT

The authors claim no conflict of interest.

DATA AVAILABILITY STATEMENT

Model code and data are available on Zenodo. <https://doi.org/10.5281/zenodo.7818845> (Wiczynski et al., 2023).

ORCID

Daniel J. Wiczynski  <https://orcid.org/0000-0003-4090-2677>

Holly V. Moeller  <https://orcid.org/0000-0002-9335-0039>

Jean P. Gibert  <https://orcid.org/0000-0002-5083-6418>

REFERENCES

- Allen, A. P., Gillooly, J. F., & Brown, J. H. (2005). Linking the global carbon cycle to individual metabolism. *Functional Ecology*, 19, 202–213.
- Bar-On, Y. M., Phillips, R., & Milo, R. (2018). The biomass distribution on earth. *Proceedings of the National Academy of Sciences of the United States of America*, 115, 6506–6511.
- Bengtsson, J., Setälä, H., & Zheng, D. W. (1996). Food webs and nutrient cycling in soils: Interactions and positive feedbacks. In G. A. Polis & K. O. Winemiller (Eds.), *Food webs: Integration of patterns & dynamics* (pp. 30–38). Springer.
- Binzer, A., Guill, C., Brose, U., & Rall, B. C. (2012). The dynamics of food chains under climate change and nutrient enrichment. *Philosophical Transactions of the Royal Society B: Biological Sciences*, 367, 2935–2944.
- Binzer, A., Guill, C., Rall, B. C., & Brose, U. (2016). Interactive effects of warming, eutrophication and size structure: Impacts on biodiversity and food-web structure. *Global Change Biology*, 22, 220–227.
- Bradford, M. A., McCulley, R. L., Crowther, T. W., Oldfield, E. E., Wood, S. A., & Fierer, N. (2019). Cross-biome patterns in soil microbial respiration predictable from evolutionary theory on thermal adaptation. *Nature Ecology and Evolution*, 3, 223–231.
- Brown, J. H., Gillooly, J. F., Allen, A. P., Savage, V. M., & West, G. B. (2004). Toward a metabolic theory of ecology. *Ecology*, 85, 1771–1789.
- Connell, J. H., & Sousa, W. P. (1983). On the evidence needed to judge ecological stability or persistence. *The American Naturalist*, 121, 789–824.
- Dakos, V., & Hastings, A. (2013). Editorial: Special issue on regime shifts and tipping points in ecology. *Theoretical Ecology*, 6, 253–254.
- Dakos, V., Matthews, B., Hendry, A. P., Levine, J., Loeuille, N., Norberg, J., Nosil, P., Scheffer, M., & de Meester, L. (2019). Ecosystem tipping points in an evolving world. *Nature Ecology and Evolution*, 3, 355–362.
- De Carvalho Braga, D., & Mello, L. F. (2013). A study of the coexistence of three types of attractors in an autonomous system. *International Journal of Bifurcation and Chaos*, 23, 1350203.
- Dell, A. I., Pawar, S., & Savage, V. M. (2011). Systematic variation in the temperature dependence of physiological and ecological traits.

- Proceedings of the National Academy of Sciences of the United States of America*, 108, 10591–10596.
- Dell, A. I., Pawar, S., & Savage, V. M. (2014). Temperature dependence of trophic interactions are driven by asymmetry of species responses and foraging strategy. *The Journal of Animal Ecology*, 83, 70–84.
- Dudney, J., & Suding, K. N. (2020). The elusive search for tipping points. *Nature Ecology and Evolution*, 4, 1449–1450.
- Eiler, A. (2006). Evidence for the ubiquity of mixotrophic bacteria in the Upper Ocean: Implications and consequences. *Applied and Environmental Microbiology*, 72, 7431–7437.
- Erbach, A., Lutscher, F., & Seo, G. (2013). Bistability and limit cycles in generalist predator–prey dynamics. *Ecological Complexity*, Special Issue on the occasion of Horst Malchow's 60th birthday, 14, 48–55.
- Esteban, G. F., Fenchel, T., & Finlay, B. J. (2010). Mixotrophy in ciliates. *Protist*, 161, 621–641.
- Flynn, K. J., Mitra, A., Anestis, K., Anschütz, A. A., Calbet, A., Ferreira, G. D., Gypens, N., Hansen, P. J., John, U., Martin, J. L., Mansour, J. S., Maselli, M., Medić, N., Norlin, A., Not, F., Pitta, P., Romano, F., Saiz, E., Schneider, L. K., ... Traboni, C. (2019). Mixotrophic protists and a new paradigm for marine ecology: Where does plankton research go now? *Journal of Plankton Research*, 41, 375–391.
- Flynn, K. J., Stoecker, D. K., Mitra, A., Raven, J. A., Glibert, P. M., Hansen, P. J., Granéli, E., & Burkholder, J. M. (2013). Misuse of the phytoplankton–zooplankton dichotomy: The need to assign organisms as mixotrophs within plankton functional types. *Journal of Plankton Research*, 35, 3–11.
- Folke, C., Carpenter, S., Walker, B., Scheffer, M., Elmqvist, T., Gunderson, L., & Holling, C. S. (2004). Regime shifts, resilience, and biodiversity in ecosystem management. *Annual Review of Ecology, Evolution, and Systematics*, 35, 557–581.
- Gao, Z., Karlsson, I., Geisen, S., Kowalchuk, G., & Jousset, A. (2019). Protists: Puppet masters of the rhizosphere microbiome. *Trends in Plant Science*, 24, 165–176.
- Geisen, S., Hu, S., dela Cruz, T. E. E., & Veen, G. F. (Ciska). (2021). Protists as catalyzers of microbial litter breakdown and carbon cycling at different temperature regimes. *The ISME Journal*, 15, 618–621.
- Geisen, S., Lara, E., Mitchell, E. A. D., Völcker, E., & Krashevska, V. (2020). Soil protist life matters! *Soil Organisms*, 92, 189–196.
- Gibert, J. P., Allen, R. L., Hruska, R. J., III, & DeLong, J. P. (2017). The ecological consequences of environmentally induced phenotypic changes. *Ecology Letters*, 20, 997–1003.
- Gilbert, B., Tunney, T. D., McCann, K. S., DeLong, J. P., Vasseur, D. A., Savage, V., Shurin, J. B., Dell, A. I., Barton, B. T., Harley, C. D. G., Kharouba, H. M., Kratina, P., Blanchard, J. L., Clements, C., Winder, M., Greig, H. S., & O'Connor, M. I. (2014). A bioenergetic framework for the temperature dependence of trophic interactions. *Ecology Letters*, 17, 902–914.
- Graham, E. R., Fay, S. A., Davey, A., & Sanders, R. W. (2013). Intracapsular algae provide fixed carbon to developing embryos of the salamander *Ambystoma maculatum*. *The Journal of Experimental Biology*, 216, 452–459.
- Han, Z.-Y., Wiczyński, D. J., Yamine, A., & Gibert, J. P. (2023). Temperature and nutrients drive eco-phenotypic dynamics in a microbial food web. *Proceedings of the Royal Society B: Biological Sciences*, 290, 20222263.
- Hillebrand, H., Donohue, I., Harpole, W. S., Hodapp, D., Kucera, M., Lewandowska, A. M., Merder, J., Montoya, J. M., & Freund, J. A. (2020). Thresholds for ecological responses to global change do not emerge from empirical data. *Nature Ecology and Evolution*, 4, 1502–1509.
- Holling, C. S. (1973). Resilience and stability of ecological systems. *Annual Review of Ecology and Systematics*, 4, 1–23.
- Jassey, V. E. J., Signarbieux, C., Hättenschwiler, S., Bragazza, L., Buttler, A., Delarue, F., Fournier, B., Gilbert, D., Laggoun-Défarge, F., Lara, E., T. E. Mills, R., Mitchell, E. A. D., Payne, R. J., & Robroek, B. J. M. (2015). An unexpected role for mixotrophs in the response of peatland carbon cycling to climate warming. *Scientific Reports*, 5, 16931.
- Jones, H. (1997). A classification of mixotrophic protists based on their behaviour. *Freshwater Biology*, 37, 35–43.
- Jones, R. I. (2000). Mixotrophy in planktonic protists: An overview. *Freshwater Biology*, 45, 219–226.
- Jost, C., Lawrence, C. A., Campolongo, F., van de Bund, W., Hill, S., & DeAngelis, D. L. (2004). The effects of mixotrophy on the stability and dynamics of a simple planktonic food web model. *Theoretical Population Biology*, 66, 37–51.
- Kayranli, B., Scholz, M., Mustafa, A., & Hedmark, Å. (2010). Carbon storage and fluxes within freshwater wetlands: A critical review. *Wetlands*, 30, 111–124.
- Kuppardt-Kirmse, A., & Chatzinotas, A. (2020). Intraguild predation: Predatory networks at the microbial scale. In E. Jurkevitch & R. J. Mitchell (Eds.), *The ecology of predation at the microscale* (pp. 65–87). Springer International Publishing.
- López-Urrutia, Á., San Martín, E., Harris, R. P., & Irigoien, X. (2006). Scaling the metabolic balance of the oceans. *Proceedings of the National Academy of Sciences of the United States of America*, 103, 8739–8744.
- May, R. M. (1977). Thresholds and breakpoints in ecosystems with a multiplicity of stable states. *Nature*, 269, 471–477.
- McCann, K. S., & Gellner, G. (2012). Food chains and food web modules. In A. Hastings & L. Gross (Eds.), *Encyclopedia of theoretical ecology* (pp. 288–294). University of California Press.
- Mieczan, T. (2009). Ciliates in sphagnum peatlands: Vertical micro-distribution, and relationships of species assemblages with environmental parameters. *Zoological Studies*, 48, 33–48.
- Mitra, A., Flynn, K. J., Burkholder, J. M., Berge, T., Calbet, A., Raven, J. A., Granéli, E., Glibert, P. M., Hansen, P. J., Stoecker, D. K., Thingstad, F., Tillmann, U., Våge, S., Wilken, S., & Zubkov, M. V. (2014). The role of mixotrophic protists in the biological carbon pump. *Biogeosciences*, 11, 995–1005.
- Mitra, A., Flynn, K. J., Tillmann, U., Raven, J. A., Caron, D., Stoecker, D. K., Not, F., Hansen, P. J., Hallegraef, G., Sanders, R., Wilken, S., McManus, G., Johnson, M., Pitta, P., Våge, S., Berge, T., Calbet, A., Thingstad, F., Jeong, H. J., ... Lundgren, V. (2016). Defining planktonic Protist functional groups on mechanisms for energy and nutrient acquisition: Incorporation of diverse mixotrophic strategies. *Protist*, 167, 106–120.
- Moeller, H. V., Neubert, M. G., & Johnson, M. D. (2019). Intraguild predation enables coexistence of competing phytoplankton in a well-mixed water column. *Ecology*, 100, e02874.
- Moeller, H. V., Peltomaa, E., Johnson, M. D., & Neubert, M. G. (2016). Acquired phototrophy stabilises coexistence and shapes intrinsic dynamics of an intraguild predator and its prey. *Ecology Letters*, 19, 393–402.
- Moroz, I. M., Cropp, R., & Norbury, J. (2019). Mixotrophs: Dynamic disrupters of plankton systems? *Journal of Sea Research*, 147, 37–45.
- Orr, H. (1888). Memoirs: Note on the development of amphibians, chiefly concerning the central nervous system; with additional observations on the hypophysis, mouth, and the appendages and skeleton of the head. *Journal of Cell Science*, s2-29, 295–324.
- Petchey, O. L., McPhearson, P. T., Casey, T. M., & Morin, P. J. (1999). Environmental warming alters food-web structure and ecosystem function. *Nature*, 402, 69–72.
- Raven, J. A. (1997). Phagotrophy in phototrophs. *Limnology and Oceanography*, 42, 198–205.
- Rocca, J. D., Yamine, A., Simonin, M., & Gibert, J. P. (2022). Protist predation influences the temperature response of bacterial communities. *Frontiers in Microbiology*, 13, 847964.
- Sanders, R. W. (1991). Mixotrophic protists In marine and freshwater ecosystems. *The Journal of Protozoology*, 38, 76–81.
- Savage, V. M., Gilloly, J. F., Brown, J. H., & Charnov, E. L. (2004). Effects of body size and temperature on population growth. *The American Naturalist*, 163, 429–441.

- Scheffer, M., Bascompte, J., Brock, W. A., Brovkin, V., Carpenter, S. R., Dakos, V., Held, H., van Nes, E. H., Rietkerk, M., & Sugihara, G. (2009). Early-warning signals for critical transitions. *Nature*, *461*, 53–59.
- Scheffer, M., Carpenter, S., Foley, J. A., Folke, C., & Walker, B. (2001). Catastrophic shifts in ecosystems. *Nature*, *413*, 591–596.
- Schimel, J., & Schaeffer, S. (2012). Microbial control over carbon cycling in soil. *Frontiers in Microbiology*, *3*, 348.
- Schmidt, S., Raven, J. A., Paungfoo-Lonhienne, C., Schmidt, S., Raven, J. A., & Paungfoo-Lonhienne, C. (2013). The mixotrophic nature of photosynthetic plants. *Functional Plant Biology*, *40*, 425–438.
- Selosse, M.-A., Charpin, M., & Not, F. (2017). Mixotrophy everywhere on land and in water: The grand écart hypothesis. *Ecology Letters*, *20*, 246–263.
- Selosse, M.-A., & Roy, M. (2009). Green plants that feed on fungi: Facts and questions about mixotrophy. *Trends in Plant Science*, *14*, 64–70.
- Sentis, A., Hemptinne, J.-L., & Brodeur, J. (2014). Towards a mechanistic understanding of temperature and enrichment effects on species interaction strength, omnivory and food-web structure. *Ecology Letters*, *17*, 785–793.
- Smith, T. P., Thomas, T. J. H., García-Carreras, B., Sal, S., Yvon-Durocher, G., Bell, T., & Pawar, S. (2019). Community-level respiration of prokaryotic microbes may rise with global warming. *Nature Communications*, *10*, 5124.
- Steinberg, D. K., & Landry, M. R. (2017). Zooplankton and the ocean carbon cycle. *Annual Review of Marine Science*, *9*, 413–444.
- Stoecker, D. K. (1998). Conceptual models of mixotrophy in planktonic protists and some ecological and evolutionary implications. *European Journal of Protistology*, *34*, 281–290.
- Stoecker, D. K., Hansen, P. J., Caron, D. A., & Mitra, A. (2017). Mixotrophy in the marine plankton. *Annual Review of Marine Science*, *9*, 311–335.
- Thakur, M. P., & Geisen, S. (2019). Trophic regulations of the soil microbiome. *Trends in Microbiology*, *27*, 771–780.
- Thingstad, T. F., Havskum, H., Garde, K., & Riemann, B. (1996). On the strategy of “eating your competitor”: A mathematical analysis of algal mixotrophy. *Ecology*, *77*, 2108–2118.
- Tyson, R., & Lutscher, F. (2016). Seasonally varying predation behavior and climate shifts are predicted to affect predator-prey cycles. *The American Naturalist*, *188*, 539–553.
- Venn, A. A., Loram, J. E., & Douglas, A. E. (2008). Photosynthetic symbioses in animals. *Journal of Experimental Botany*, *59*, 1069–1080.
- Wieczynski, D. J., Moeller, H. V., & Gibert, J. P. (2023). Code and data from “Mixotrophic microbes create carbon tipping points under warming”. *Zenodo*.
- Wieczynski, D. J., Singla, P., Doan, A., Singleton, A., Han, Z.-Y., Votzke, S., Yamine, A., & Gibert, J. P. (2021). Linking species traits and demography to explain complex temperature responses across levels of organization. *Proceedings of the National Academy of Sciences of the United States of America*, *118*, e2104863118.
- Wilken, S., Huisman, J., Naus-Wiezer, S., & Donk, E. V. (2013). Mixotrophic organisms become more heterotrophic with rising temperature. *Ecology Letters*, *16*, 225–233.
- Wilken, S., Soares, M., Urrutia-Cordero, P., Ratcovich, J., Ekvall, M. K., Donk, E. V., & Hansson, L.-A. (2018). Primary producers or consumers? Increasing phytoplankton bacterivory along a gradient of lake warming and browning. *Limnology and Oceanography*, *63*, S142–S155.
- Wolfram Research Inc. (2021). Mathematica version 13.0.0, Champaign, Illinois.
- Worden, A. Z., Follows, M. J., Giovannoni, S. J., Wilken, S., Zimmerman, A. E., & Keeling, P. J. (2015). Rethinking the marine carbon cycle: Factoring in the multifarious lifestyles of microbes. *Science*, *347*(6223), 1257594.
- Yafremava, L., Wielgos, M., Thomas, S., Nasir, A., Wang, M., Mittenthal, J., & Caetano-Anollés, G. (2013). A general framework of persistence strategies for biological systems helps explain domains of life. *Frontiers in Genetics*, *4*, 16.
- Yang, Z., Zhang, L., Zhu, X., Wang, J., & Montagnes, D. J. S. (2016). An evidence-based framework for predicting the impact of differing autotroph-heterotroph thermal sensitivities on consumer-prey dynamics. *The ISME Journal*, *10*, 1767–1778.
- Yvon-Durocher, G., & Allen, A. P. (2012). Linking community size structure and ecosystem functioning using metabolic theory. *Philosophical Transactions of the Royal Society B: Biological Sciences*, *367*, 2998–3007.
- Zhang, C., Dang, H., Azam, F., Benner, R., Legendre, L., Passow, U., Polimene, L., Robinson, C., Suttle, C. A., & Jiao, N. (2018). Evolving paradigms in biological carbon cycling in the ocean. *National Science Review*, *5*, 481–499.
- Zhou, J., Xue, K., Xie, J., Deng, Y., Wu, L., Cheng, X., Fei, S., Deng, S., He, Z., van Nostrand, J. D., & Luo, Y. (2012). Microbial mediation of carbon-cycle feedbacks to climate warming. *Nature Climate Change*, *2*, 106–110.

SUPPORTING INFORMATION

Additional supporting information can be found online in the Supporting Information section at the end of this article.

Figure S1. Functional forms of functional responses for photosynthesis and predation rates across (a) prey densities, (b) nutrient concentrations and (c) temperatures for a Type-IIIa ‘phototrophic protozoa’ mixotroph (following [Stoecker, 1998]).

Figure S2. (a–c) Functional forms of functional responses for photosynthesis and predation rates across (a) prey densities, (b) nutrient concentrations and (c) temperatures for a Type-IIa ‘phagotrophic algae’ mixotroph (following [Stoecker, 1998]). (d) Equilibrium mixotroph density and CO₂ flux as a function of temperature in this Type-IIa mixotroph where all parameter values are the same as those used in the main analysis of a Type-IIIa mixotroph (Table 1) except $\mu_M(T)$: $b_0=1.3$, $\mu_P(T)$: $b_0=0.34$, $\alpha(T)$: $b_0=0.65$ and $K_p=27$. Two new functions have been added to accommodate Type-IIa mixotrophic dynamics: (1) a positive, saturating relationship between photosynthetic rate and prey density $P/(h_{MP}+P)$ with $h_{MP}=2$, and (2) negative relationship between predation rate and nutrient concentration $e^{-d_{N_M} N_M^2}$ with $d_{N_M}=5$. Colours, line types and shading are the same as in Figures 3 and S1.

Figure S3. Equilibrium mixotroph density and CO₂ flux as a function of temperature when the temperature sensitivities of photosynthesis and predation are the same ($\mu_M(T)$: $E_a=0.65$, $\mu_P(T)$: $E_a=0.65$). All other parameter values are the same as those used in the main analysis of a Type-IIIa mixotroph (Table 1) except $\mu_M(T)$: $b_0=0.43$. Colours, line types and shading are the same as in Figure 3.

Figure S4. Equilibrium mixotroph densities and net CO₂ flux shown across temperatures and across gradients of nutrient concentrations for nutrients utilized by a mixotroph (vertical) and its prey (horizontal). The centre column corresponds to panels c–e in Figure 3 in the main text. Colours, line types and shading are the same as in Figure 3.

Figure S5. Equilibrium phase space shown for a variation of our mixotrophy model that includes dynamic nutrients for the mixotroph (i.e. N_M is treated as a state variable with its own differential equation).

Orange, blue and green surfaces correspond to prey, mixotroph and nutrient null clines. Intersections of these null clines represent equilibrium points (solid green and orange dots) and the blue line indicates stable limit cycles that orbit the interior equilibria (as in Figure 2 in the main text). Although the nutrient dimension introduces more complex equilibria that include fluctuating nutrient concentrations, the results here are qualitatively the same as in the static nutrient model. In this version of the model, nutrients utilized by the mixotroph follow chemostat dynamics, with reduction due to mixotroph photosynthetic production: $\frac{dN_M}{dt} = \theta(N_{M,feed} - N_M) - M * \varphi(T, N_M, P, M)$, where N_M is the concentration of nutrients utilized by the mixotroph, θ is a dilution rate, $N_{M,feed}$ is a feed concentration for mixotroph nutrients, M is mixotroph density and φ is the per-capita photosynthetic production rate of the mixotroph. Nutrient model parameters used for the results shown here were $\theta = 10 \text{ mg L}^{-1} \text{ t}^{-1}$ and $N_{M,feed} = 0.75 \text{ mg L}^{-1}$. All other model parameters were the same as used in the main results (Table 1).

Figure S6. Sensitivity analysis showing the relative sensitivities of equilibrium mixotroph density to 50% increases (blue) and 50% decreases (red) in each parameter listed in Table 1. In each panel, solid lines denote fixed point equilibria, dashed lines denote unstable foci, grey regions denote stable limit cycles (fluctuations), and dotted lines denote unstable saddle points. Results here assume intermediate nutrient concentrations $N_M = 0.7 \text{ mg L}^{-1}$.

How to cite this article: Wiczynski, D. J., Moeller, H. V., & Gibert, J. P. (2023). Mixotrophic microbes create carbon tipping points under warming. *Functional Ecology*, 00, 1–13. <https://doi.org/10.1111/1365-2435.14350>